Coupled Mode Analysis of Metal-Insulator-Metal Waveguide Coupled with a Resonant Cavity

Tomotaka Ikeda[1], Toshiaki Kitamura[2], Kiyoshi Kishioka[3]

[1,2]Kansai UNIVERSITY, 3-3-35 Yamate-cho, Suita-shi, 564-8680 Japan
[3]Osaka Electro-Communication UNIVERSITY, 18-8 Hatsu-cho, Neyagawa-shi, 572-8530 Japan
[1]k712186@kansai-u.ac.jp, [2]kita@kansai-u.ac.jp, [3]kishioka@isc.osakac.ac.jp

The coupling coefficients of two parallel metal-insulator-metal (MIM) plasmonic waveguides are investigated using the analysis of the coupled-mode equations. The frequency characteristics of the power transmittance of a MIM waveguide coupled with a resonant cavity are also studied and compared with the simulation results obtained from the FDTD method into which motion equations of free electrons are installed.

***Index Terms* — Plasmons, coupled mode analysis, metal-insulator structures, optical waveguides.**

I. Introduction

Surface plasmon polaritons (SPPs), which are transverse-magnetic waves that propagate along the metal and dielectric interface, have attracted much interest due to their ability to manipulate light at a subwavelength scale. Planar SPP devices mainly consist of two types of configurations, metal-insulator-metal (MIM) and insulator -metal-insulator (IMI). Among these structures, MIM configurations have been attracting much attention because they have advantages due to their strong field localization and easiness of fabrication. According to this, various MIM plasmonic devices have been proposed so far, such as ring resonators [1], Bragg gratings [2], splitters and demultiplexers [3], filters utilizing cascaded transverse cavities [4] and so on. Analytical modeling of resonant cavities for MIM waveguide junctions has also been investigated [5]. Most of these studies have utilized FDTD simulation to investigate the characteristics.

In this study, we deal with a MIM resonant cavity coupled with a MIM waveguide by using the coupled-mode theory [6] which can analyze the characteristics while saving the computer resources. The frequency characteristics of the power transmittance of a MIM waveguide coupled with a resonant cavity are also studied and compared with the simulation results. The simulations are carried out by using the FDTD method into which motion equations of free electrons (Drude model) are installed [7].

II. Metal-Insulator-Metal Waveguide

Figure 1 shows a MIM waveguide coupled with a resonant cavity. Here, it is assumed that the cavity has the same width ($2a$) as the waveguide and the length along the propagation direction is L.

First, we describe the fundamental propagation modes of a MIM waveguide which consists of silver and air. In this study, we deal with silver as ideal metal which has the dielectric function of the undamped free electron plasma.

When we consider the fundamental transverse-magnetic (TM) mode of the MIM waveguide, the electromagnetic fields of each region are described by the following equations:

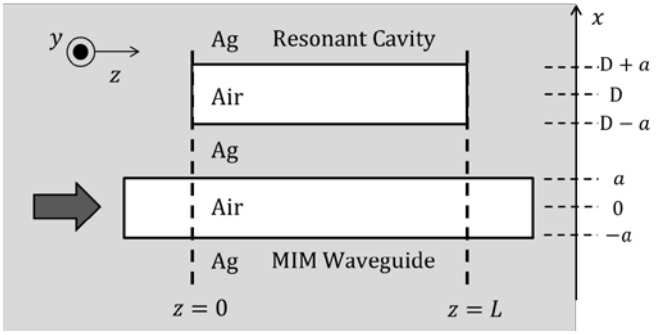

Fig.1. MIM waveguide coupled with a resonant cavity.

$$\begin{cases} H_y = \mathrm{A}e^{-k_2 x}e^{-j\beta z} \\ E_x = \mathrm{A}\dfrac{\beta}{\omega\varepsilon_0\varepsilon_2}e^{-k_2 x}e^{-j\beta z} \\ E_z = j\mathrm{A}\dfrac{k_2}{\omega\varepsilon_0\varepsilon_2}e^{-k_2 x}e^{-j\beta z} \end{cases} \quad (1)$$

for $x > a$ and

$$\begin{cases} H_y = \mathrm{A}e^{k_2 x}e^{-j\beta z} \\ E_x = \mathrm{A}\dfrac{\beta}{\omega\varepsilon_0\varepsilon_2}e^{k_2 x}e^{-j\beta z} \\ E_z = -j\mathrm{A}\dfrac{k_2}{\omega\varepsilon_0\varepsilon_2}e^{k_2 x}e^{-j\beta z} \end{cases} \quad (2)$$

for $x < -a$, and

$$\begin{cases} H_y = \mathrm{B}(e^{k_1 x} + e^{-k_1 x})e^{-j\beta z} \\ E_x = \mathrm{B}\dfrac{\beta}{\omega\varepsilon_0\varepsilon_1}(e^{k_1 x} + e^{-k_1 x})e^{-j\beta z} \\ E_z = -j\mathrm{B}\dfrac{k_1}{\omega\varepsilon_0\varepsilon_1}(e^{k_1 x} - e^{-k_1 x})e^{-j\beta z} \end{cases} \quad (3)$$

for $-a < x < a$,

where k_i and ε_i (i=1, 2) represent the wavenumbers along the x axis and the relative permittivity, respectively, of each region.

III. Coupling Coefficients

The coupling coefficient of the two parallel MIM waveguides is given by [8]

$$c = \frac{\omega\varepsilon_0(\varepsilon_2 - \varepsilon_1)\int_{-a}^{a} \boldsymbol{E_1}^* \cdot \boldsymbol{E_2} dx}{\int_{-\infty}^{\infty} \boldsymbol{u_z} \cdot (\boldsymbol{E_1}^* \times \boldsymbol{H_1} + \boldsymbol{E_1} \times \boldsymbol{H_1}^*)\, dx}, \quad (4)$$

where,

$$\boldsymbol{E_1}^* \cdot \boldsymbol{E_2} = \frac{1}{\omega^2 {\varepsilon_0}^2 \varepsilon_2}\left(\beta^2 {H_{1y}}^* H_{2y} + \frac{\partial {H_{1y}}^*}{\partial x}\frac{\partial H_{2y}}{\partial x}\right)$$

and

$$\boldsymbol{u_z} \cdot (\boldsymbol{E_1}^* \times \boldsymbol{H_1} + \boldsymbol{E_1} \times \boldsymbol{H_1}^*) = \frac{2\beta}{\omega\varepsilon_0 \varepsilon}\left|H_{1y}\right|^2.$$

where H_{1y} in each region is calculated from the equations (1)-(3) and H_{2y} is equal to $Ae^{k_2(x-\mathrm{D})}e^{-j\beta z}$.

Figure 2 shows the coupling coefficients as a function of the incident wavelength. Here, the half width of the waveguides a = 25[nm]. We have confirmed that the coupling coefficients coincide with the ones which are obtained from the propagation constants of even and odd modes [8]: $c = (\beta_{\text{even}} - \beta_{\text{odd}}) / 2$.

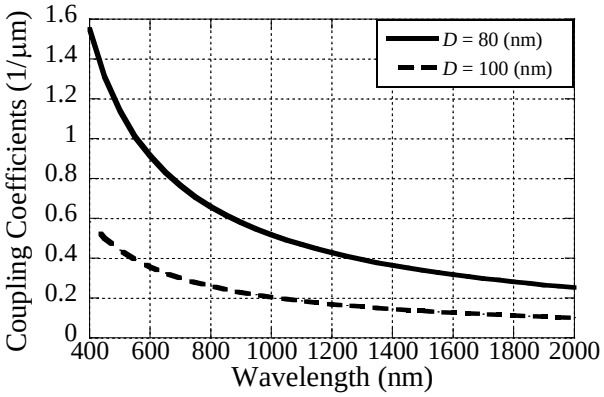

Fig.2. Coupling coefficients as a function of incident wavelength.

IV. Characteristics of Transmittance

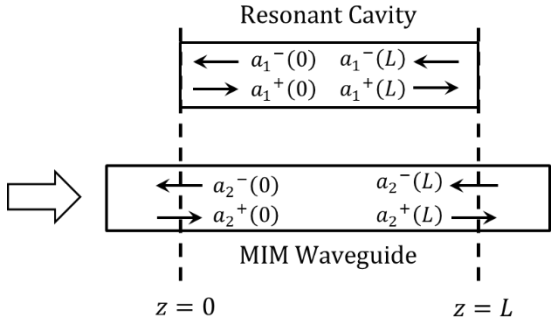

Fig.3. Field amplitudes at boundaries.

The field amplitudes of the forward and backward waves are defined as shown in Figure 3. The amplitudes are related to each other as [9]

$$\begin{aligned} \boldsymbol{a}^+(L) &= e^{-j\beta L}\hat{\mathbf{F}}(L)\boldsymbol{a}^+(0) \\ \boldsymbol{a}^-(0) &= e^{-j\beta L}\hat{\mathbf{F}}(L)\boldsymbol{a}^-(L). \end{aligned} \quad (5)$$

The components $f_{ij}(L)$ (i,j=1,2) of the transfer matrix $\hat{\mathbf{F}}(L)$ are calculated by using the coupling coefficient as follows: $f_{12}(L) = f_{21}(L) = -j \sin cL$, $f_{11}(L) = f_{22}(L) = \cos cL$. By using ${a_2}^+(L)$ and ${a_2}^+(0)$, the power transmittance $|T|^2$ is calculated as

$$|T|^2 = \left|\frac{{a_2}^+(L)}{{a_2}^+(0)}\right|^2 = \frac{\cos^2 cL\left|1 - \Gamma^2 e^{-j2\beta L}\right|^2}{\left|1 - \Gamma^2 \cos^2 cL\, e^{-j2\beta L}\right|^2}, \quad (6)$$

where, Γ is a reflection coefficient which is calculated by assuming the plane wave reflection at the boundaries between the cavity and the metal.

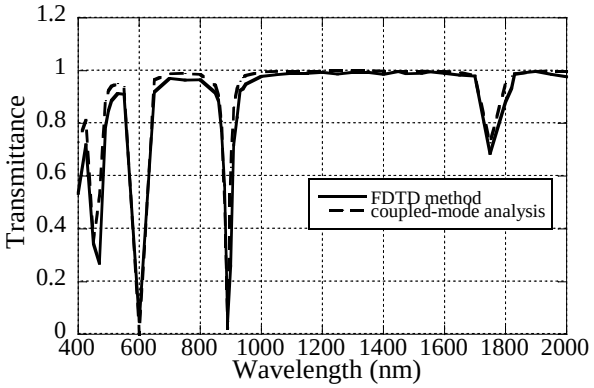

Fig.4. Power transmittance as a function of incident wavelength.

Figure 4 shows the power transmittance as a function of the incident wavelength. The results are obtained from the coupled mode analysis and the FDTD simulation, respectively. Here, the structural parameters are chosen as follows: a = 25[nm], D = 80[nm], L = 600[nm]. In the FDTD analysis, 5[nm] × 5[nm] square meshes are used and the PML absorbing boundaries are utilized to truncate the computational domain.

It is understood from this figure that the bandstop filtering characteristics, which have several stopband frequencies, can be obtained. It is also confirmed that the results from the coupled mode analysis and the FDTD simulation show a good agreement with each other.

V. References

[1] A. Hosseini and Y. Massoud, "Nanoscale surface plasmon based resonator using rectangular geometry," *Appl. Phys. Lett.*, 90, 181102, 2007.

[2] Y. J. Chang and G. Y. Lo, "A narrowband metal-insulator-metal waveguide plasmonic Bragg grating," *IEEE Photon. Technol. Lett.*, vol. 22, no. 9, pp.634-636, May 2010.

[3] J. H. Zhu, X. G. Huang, and X. Mei, "Improved models for plasmonic waveguide splitters and demultiplexeres at the telecommunication wavelengths," *IEEE Trans. Nanotechnol*., vol. 10, no. 5, pp.1166-1171, Sept. 2011.

[4] L. O. Diniz, F. D. Nunes, E. Marega, J. Weiner, and B. V. Borges, "Metal-insulator-metal surface plasmon polariton waveguide filters with cascaded transverse cavities," *J. LightwaveTechnol*., vol. 29, no. 5, pp.714-720, Mar. 2011.

[5] A. Pannipitiya, I. D. Rukhlenko, and M. Premaratne, "Analytical modeling of resonant cavities for plasmonic-slot-waveguide junctions," *IEEE Photon. J.*, vol. 3, no. 2, pp. 220-233, Apr. 2011.

[6] K. Kishioka, "A design method to achieve wide wavelength-flattered responses in the directional coupler-type optical power splitters," *J. Lightwave Technol*., vol. 19, no. 11, pp.1705-1715, Nov. 2001.

[7] T. Kitamura, "FDTD analysis of a near-field optical disk with a ridged-square nano-aperture," *IEICE Trans. Electron*., vol. E95-C, no. 6, pp.1110-1116, June 2012.

[8] D. Marcuse, Light Transmission Optics, chapter 10, Van Nostrand Reinhold, New York, 1972.

[9] K. Kishioka, "Characteristics of the optical resonator composed of the nonlinear directional coupler," *IEEJ Trans. FM*., vol.123, no.12, pp1166-1173, 2003.